International Journal of Electrical Engineering.
ISSN 0974-2158 Volume 4, Number 1 (2011), pp.59-74

http://www.irphouse.com

Modeling of Conducted EMI in Switching Power Converters using Equivalent Circuit Model

R. Vimala[1], K. Baskaran[2] and K.R. Aravind Britto[3]

[1]*Dept. of EEE, PSNACET, Dindigul, Tamil Nadu–624 005, India*
E-mail: vimala79@rediffmail.com
[2]*Member IEEE, M.I.S.T.E., Dept. of CSE, GCT, Coimbatore, Tamil Nadu, India.*
E-mail: baski_101@yahoo.com
[3]*Dept. of ECE, RVSCET, Dindigul, Tamil Nadu–624 005, India.*
E-mail: krbritto@yahoo.com

Abstract

This paper proposes a simple equivalent circuit modeling approach for describing EMI coupling mechanisms in switching power converters. The resulting model assumes a minimum number of noise sources and contains essential coupling paths that allow easy physical interpretations. The analytical MM noise model is first investigated to get a full understanding of the EMI mechanism. The EMI characteristics of the converters can be analytically deduced from a circuit theoretical viewpoint. Three modes of conducted EMI noise: the mixed-mode (MM), the intrinsic-differential-mode (IDM), and the common-mode (CM) are identified by time domain measurements associated with an isolated half-bridge ac–dc converter. The procedure of parameters estimation for the noise models comprises simple measurements and is convenient to be implemented. Experimental results are also included to verify the validity of the proposed method. Being based on an equivalent circuit approach, the proposed model is easy to apply in practice for understanding, diagnosing and approximating EMI behaviors.

Keywords*:* Conducted electromagnetic interference, equivalent circuit models, noise sources and impedances, switching power converters, coupling paths, modeling.

Introduction

Accurate modeling of EMI noise generation and propagation in power converters is the first step to predicting and managing the EMI noise in a system. Recent research shows that the switching power modules are the noise emission sources. The effective EMI prediction often relies on the engineer's experience or extensive numerical simulation models [1]–[3]. The diagnosis and modeling method of noise sources and coupling paths is helpful for designers in improving the converters' electromagnetic compatibility (EMC) performance. Many different methods have been proposed for parasitic modeling such as the three-dimensional (3-D) finite element analysis, time-domain reflectometry (TDR) [4], and the partial element equivalent circuit (PEEC) method [5]. Equivalent circuit models are proven to be adequate for analysis and prediction of EMI behaviors up to around 30 MHz [6]–[11]. This model contains all essential coupling paths that should be taken into consideration when evaluating the level of EMI that can be picked up by the standard line-impedance-stabilization-network (LISN).

The CM and DM excitation sources are measured online and Thevenin impedances can be measured offline, thus the pulse width modulated (PWM) drive or power converter system can be represented as a simple equivalent circuit model. The EMI modeling techniques for power converters need to be extended to include noise coupling phenomena in switching power converters [12]–[14]. In power electronics converters, the major EMI source is associated with the high dv/dt and di/dt during the switching instant. Another paper is presented for modeling the EMI source by theoretical modeling method considering the switching transient modeling, which is shown that the high frequency noise is modeled with an acceptable accuracy [15]. The DM (MM and IDM) and CM filters can be assembled together to get a complete EMI filter. The detailed process was introduced in [16] and one can followed the flow chart of the filter design method presented by Sheng [17]. The paper is organized as follows. In Section II, the derivation of the model based on a circuit theoretic viewpoint is presented. An illustration of the equivalent circuit model is given in Section III. In Section IV, an illustration of the procedure for estimating the parameters for the model is given along with an experimental verification of the viability of equivalent circuit representation for EMI prediction.

EMI Generation and Essential Coupling Paths

Conducted EMI Measurement

Fig. 1 shows the configuration of the conducted EMI measurement for an isolated half-bridge ac–dc converter. The power source is provided through a line impedance stabilizing network (LISN), which is required by the conducted EMI measurement and contains inductors, capacitors, and resistors. For power-line frequency, the inductors are essentially short, the capacitors are essentially open, and the power passed through to supply the test system. According to conventional theory, DM noise is defined as the voltage difference between the two LISN resistors, i.e., $V_X - V_Y$ and CM noise is defined as the average voltage of the two LISN resistors, i.e., $(V_X+V_Y) / 2$.

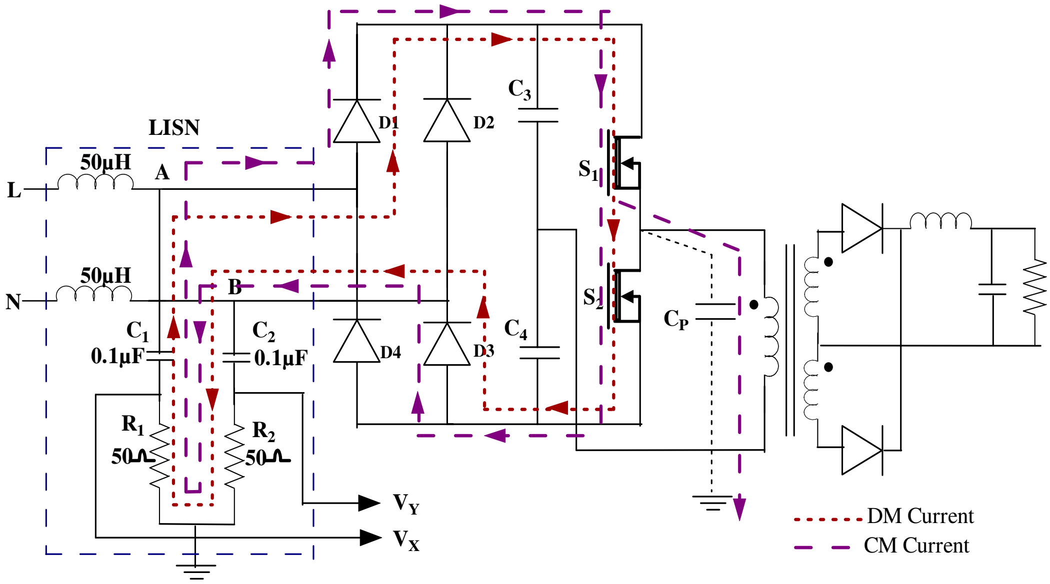

Figure 1: Half-bridge isolated ac–dc converter with EMI test setup.

For conducted EMI noise frequency, two 50μH inductors present high impedances and two 0.1μF capacitors present small impedances. The voltages measured across the two 50Ω impedances are defined by the conducted EMI, Vx is the line-side EMI, and Vy is the neutral-side EMI. DM noise voltage and CM noise voltage are expressed as

$$V_{CM} = (V_X + V_Y)/2 \tag{1}$$

$$V_{DM} = (V_X - V_Y)/2 \tag{2}$$

During normal operation, dc link is clamped at a fixed voltage by the capacitances C_3 and C_4. When ac side line voltage is larger than the capacitance voltage, the diode bridge is ON, and when line voltage is smaller than the capacitance voltage, the diode bridge is OFF. The measured DM noise fluctuates with time because of the rectifier diodes ON and OFF during half a supply cycle. But CM noise is independent of the conduction state of the rectifier. The DM noise is higher when the rectifier is OFF than that when pair of rectifier diodes are conducting.

Simplification of the Converter Circuit

Investigation has shown that equivalent circuit models contain essential noise sources and coupling paths are adequate for the analysis and prediction of the conducted EMI behaviors up to 30 MHz. The stray capacitance existing between the MOSFET and the heat sink, and the heat sink is normally connected to the ground for safety reasons. The MOSFET is mounted in the heat sink with an electrical insulating material. To make the thermal resistance small, the insulating layer is normally made as thin as possible and so a fairly large capacitance between the switching device and the ground is expected. The parasitic capacitance Cp placed between the middle point of the switching cell and the ground, as shown in Fig. 2. During normal operation, the capacitances C3 and C4 clamp the dc link voltage at a fixed value, so they can be modeled as two dc voltage sources. Since C3 = C4, V1 = V2. In the following analysis, the EMI measurement ground as the reference point. When S1 and S2 are both on OFF state, VF=VD=0, VC=V1, VE=-V2, VA=VS/2 and VB=-VS/2. The overall noise is equal to the sum of all components from individual analysis for all harmonics for a linear model.

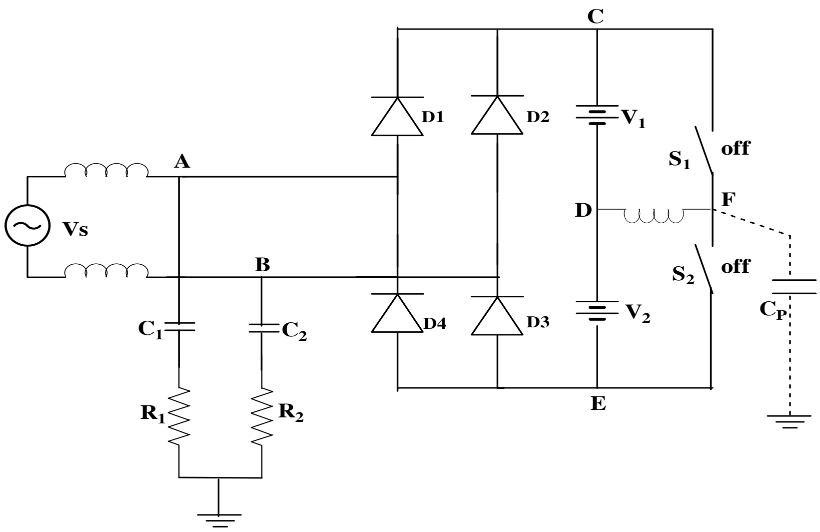

Figure 2: Simplified circuit model of the converter.

MM Noise Coupling Mode

MM noise caused by ground current is a phenomenon existing in every power converter. The mechanism of MM noise is similar to common mode noise; both depend heavily on parasitic capacitances. The term "non-intrinsic" is used to distinguish the DM emission mechanism from the "intrinsic" DM that exists when there is absolutely no ground. MM is also termed as Non-intrinsic Differential Mode (NIDM) noise. MM noise occurs due to current unbalance in the LISN branches. This mode of conducted EMI during the positive half cycle of the line voltage. This means diodes D_1 and D_3 are reverse biased, rectifier is OFF. When S_1 and S_2 are both at OFF positions, V_F is originally at zero potential. When S_1 goes to the ON position, node F is clamped to V_C instantly, resulting in charging of C_p through R_1, D_1, S_1 and $C_{p.}$ Now $V_C \approx V_A = V_S/2$, so V_E has to equal to V_C-(V_1+V_2), which is now equal to V_A› (V_1+V_2), which is less than -V_S/2. This means V_E ‹V_B‹V_A, D_2 and D_4 are reverse biased. Since only D_1 conducting, there is noise current flowing through only one branch of LISN. When S_2 goes to the ON position, node F is clamped to V_E instantly, resulting in discharging of C_p through C_p, S_2, D_3, and R_2.

Now $V_E \approx V_B$ = -V_S/2, so V_C has to equal to V_E + (V_1+V_2), which is now equal to

V_B + (V_1+V_2), which is more than $V_S/2$. This means $V_C › V_A › V_B$, D_1 and D_3 are reverse biased. There is only one diode D3 conducting this time. Switching operation of S_1 generates high-voltage change rates (dv/dt), causing negative (V_X is negative) noise current flowing through R_1, however, no current flowing through R_2,V_Y = 0. DM noise is V_{DM} = -V_X /2, CM noise is V_{CM} = -V_X /2. Switching operation of S_2 generates high-voltage change rates (dv/dt), causing positive (V_Y is positive) noise current flowing through R_2, and now no current flowing through R_1, V_Y =0. DM noise is V_{DM} = -V_Y /2, CM noise is V_{CM} = -V_Y / 2. The measured voltage V_{S1} does not stay a fixed level when both the switches are OFF state, i.e.V_{S1} changes as a slow slope before S_1 or S_2 is turned ON. Because of the unbalanced current flow through two branches of the LISN, DM noise, and CM noise are both measured. This DM is different from the conventional DM coupling because it is not related to the input power current flow but related to the charging and discharging current of C_P. The mode of EMI was then called MM in recent studies [13], [14].

IDM Noise Coupling Mode

A pulsating or harmonic rich input current causes Intrinsic Differential Mode Noise. It exists even when there is absolutely no ground. The pure DM noise, which is generated during ON state of the rectifier is called IDM noise. This means diodes D_1 and D_3 are forward biased, and the rectifier is ON. When S_1 goes to the ON position, switching operation generates high-current slew rates on the primary side of the output transformer, causing noise current flowing through R_1, D_1, C_1, C_2, D_3, and R_2 and also current flows through switch S_1. When S_2 goes to the ON position, switching operation generates high-current slew rates on the primary side of the output transformer, causing noise current flowing through R_1, D_1, C_1, C_2, D_3, and R_2 and also current flows through switch S_2.

CM Noise Coupling Mode

CM noise is directly related to stray capacitance (common mode capacitance). The CM currents are equal in phase on the hot line and the return. CM currents return to the source via the system ground. CM noise is dominant at frequency range greater than 2 MHz until 30 MHz. In this mode diodes $D_1$and D_3 are forward biased, and the rectifier is ON state. When S_1 and S_2 are both at OFF positions, the voltage at point F, V_F is originally at zero potential. When S_1 goes to the ON position, node F is clamped to V_C instantly, V_C finds two paths to charge 1) C_p, R_1, D_1, S_1, C_p and 2) R_2, D_3, C_2, C_1, S_1, C_p.

When S_2 goes to the ON position, node F is clamped to V_E instantly, resulting in the discharge of C_p through two paths 1) C_p, S_2, D_3, R_2 and 2) C_p, S_2, C_2, C_1, D_1, R_1. Regardless of whether S_1 or S_2 is switching ON, there exist two paths with almost identical impedance. The two flowing currents through the ISN branches are almost the same. This constitutes a pure CM noise coupling and no DM noise is generated due to this phenomenon. When S_1 is turned ON, V_{CM} = -V_X/2= -V_Y/2, when S_2 is turned ON, V_{CM} = -V_X/2= -V_Y/2. CM noise deduced here same as the results analyzed in MM case. This phenomenon also confirm that why CM noise is independent of the conduction state of the rectifier.

Equivalent Circuit Model for Conducted EMI

Fig. 3 shows an equivalent circuit model for description of the MM, the IDM, and the CM noise coupling paths between the converter's and the LISNs physical terminals. A linear model for the converter physical circuit consists of a simple combination of impedance elements together with voltage sources. Dealing with the EMI noise in this way, all details of the internal responses with the converter is lost, and only the external responses at the LISN input terminals are maintained. The EMI coupled from three voltage sources through three impedances, i.e., V1 and Z1 are MM coupling, V2 and Z2 are IDM coupling, and V3 and Z3 are CM coupling.

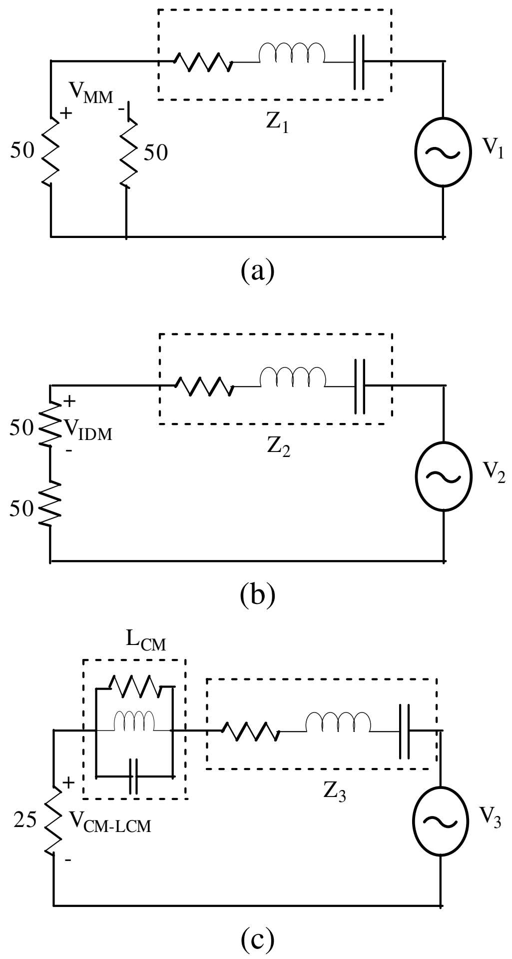

Figure 3: Equivalent circuit models of (a) MM noise (b) IDM noise (c) CM noise.

These voltage sources and impedances depend on the high dv/dt and high di/dt slew rates and circuit parasitic parameters, device package, and layout. Therefore, there are three coupling impedances associated with the different mode of the EMI, i.e., Z1 Z2, and Z3. They can be approximated by the corresponding RLC circuits in this issue. Model the noise excitation sources as Thevenin equivalent voltages V1, V2, and V3, which are terminal voltages measured at the corresponding open points of the converter. The component values of the RLC circuits are given in Table I.

Table I: Parameters Values of the Equivalent Circuit Models

Symbol	Component values of the RLC circuits		
	R	L	C
Z_1	15Ω	900nH	150pF
Z_2	5Ω	800nH	120µF
Z_3	13Ω	600nH	165pF
C_x	20mΩ	60nH	120nF
L_{CM}	50Ω	10mH	10pF

From the models shown in Fig. 3, the noise voltages of three modes can be written in terms of the equivalent noise voltage sources and coupling impedances.

$$V_{MM}(\omega) = \frac{50V_1(\omega)}{50 + Z_1(\omega)} \tag{3}$$

$$V_{IDM}(\omega) = \frac{50V_2(\omega)}{100 + Z_2(\omega)} \tag{4}$$

$$V_{CM}(\omega) = \frac{25V_3(\omega)}{25 + Z_3(\omega)} \tag{5}$$

Parameter Estimation and EMI Prediction

The estimation of the parameters in described model, and the significance of each coupling path in producing conducted EMI are illustrated in this section. The equivalent noise voltage sources, V_1 and V_2, represent the fast dv/dt impacted on C_p, are the same. The only difference between the two modes is that their coupling impedances, Z_1 and Z_3, are different. Impedance Z_1 is the impedance between point A and the ground by shorting D_1 and S_1. DM impedance Z_2 is measured between point A and B by shorting D_1, D_3 and S_1. Z_3 is the impedance between AB and the ground by shorting D_1, D_3 and S_1.

Once the noise equivalent circuits for the converter system are known, it is also possible to predict the noise EMI when filters are introduced between the converter and LISN. To investigate this, a simple filter element was included in the experimental setup. For conventional filtering design, using X capacitance to suppress DM (MM and IDM) noise, and CM choke to suppress CM noise, setup are shown in Fig.4. The actual impedance performances of the filter's elements are measured by Agilent 4294A impedance analyzer, and the impedance curves are shown in Fig. 5. The derived spectrum of the noise source without filter is shown in Fig. 6.

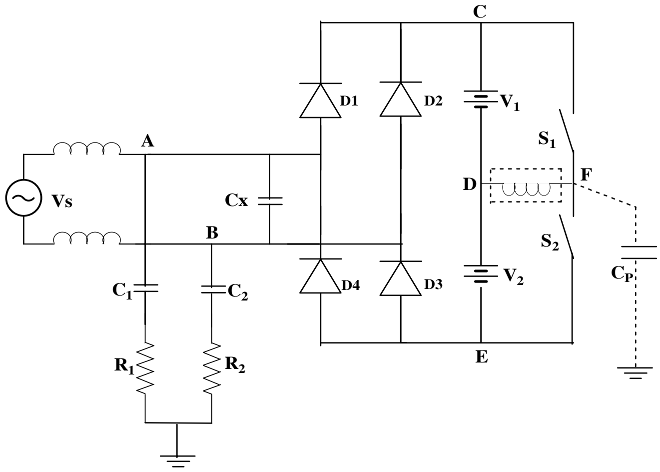

(a)

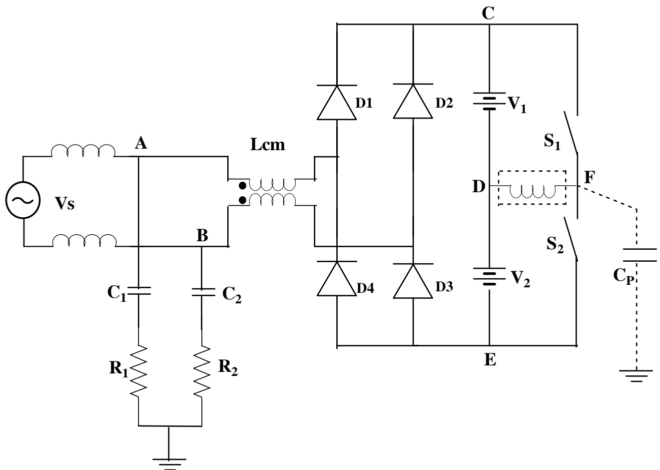

(b)

Figure 4: Filter setup of (a) an X capacitance and (b) CM chokes.

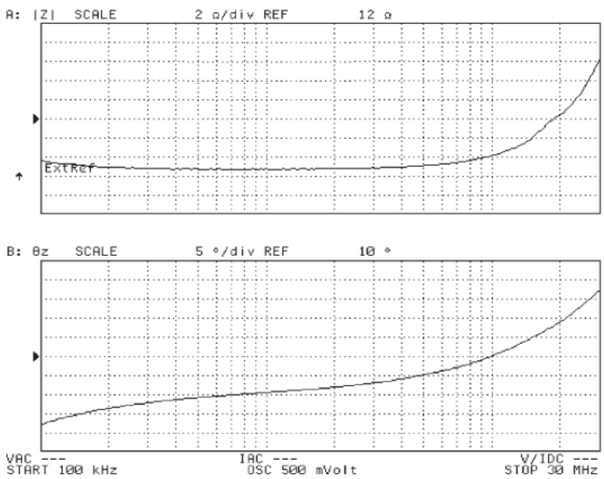

(a)

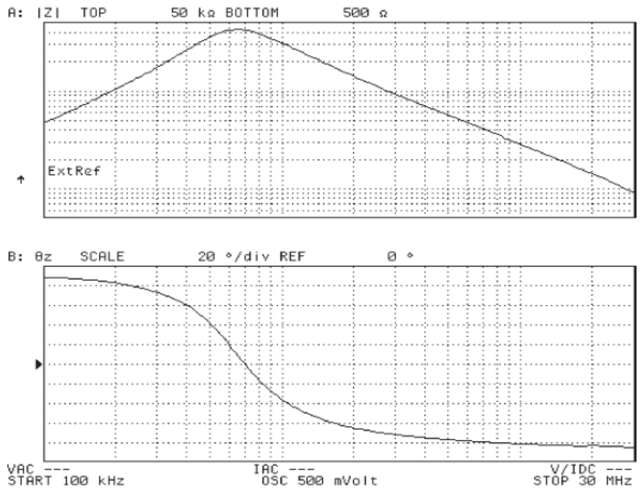

(b)

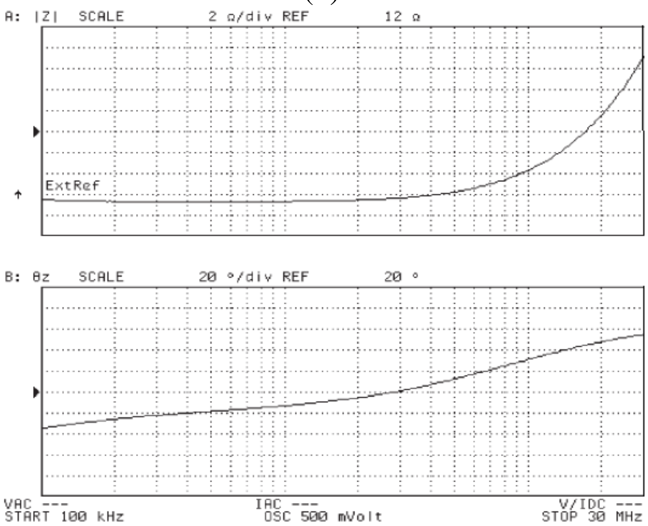

(c)

Figure 5: Measured impedances. (a) MM noise. (b) IDM noise. (c) CM noise.

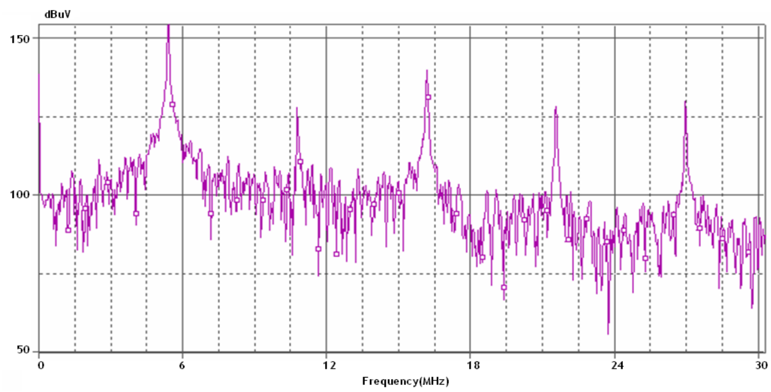

Figure 6: Derived spectra of the noise source.

The measured spectra for conducted EMI coupling path without filter is shown in Fig. 7. Thus, based on the models in Fig. 3, the MM, IDM, and CM equivalent circuits with filter in place are shown in Fig. 8. Equations (3) - (5) can be modified to compute noise voltages as

$$V_{MM-Cx}(\omega) = \frac{50Cx(\omega)V_1(\omega)}{Z_1(\omega)(100+Cx(\omega))+50(50+Cx(\omega))} \tag{6}$$

$$V_{IDM-Cx}(\omega) = \frac{50Cx(\omega)V_2(\omega)}{Z_2(\omega)(100+Cx(\omega))+100Cx(\omega)} \tag{7}$$

$$V_{CM-L_{CM}}(\omega) = \frac{25V_3(\omega)}{Z_3(\omega)+L_{CM}(\omega)+25} \tag{8}$$

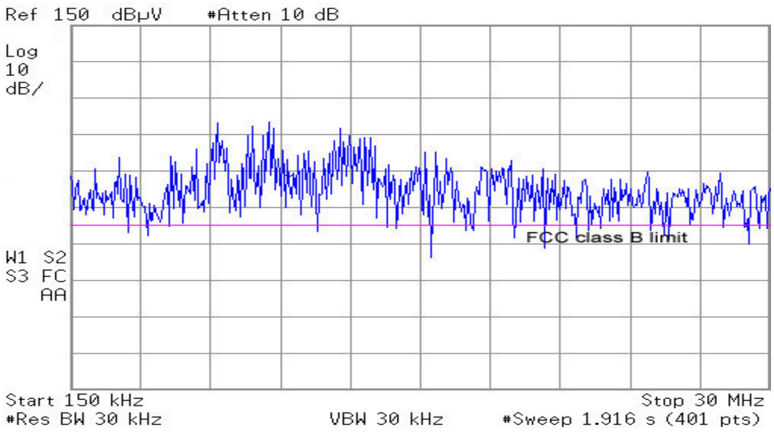

Figure 7: Measured spectra for conducted EMI coupling path without filter.

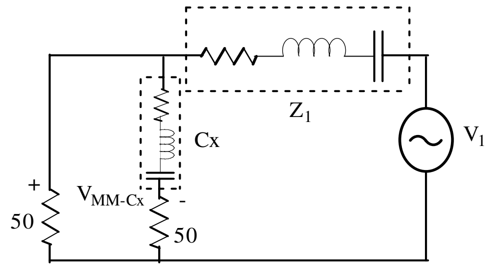

(a)

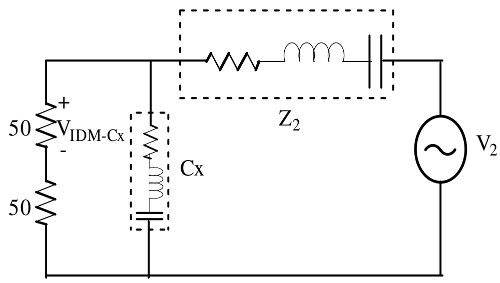

(b)

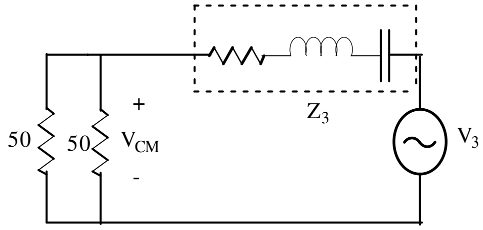

(c)

Figure 8: Equivalent circuit models with EMI filter. (a) MM noise. (b) IDM noise. (c) CM noise.

Fig. 9 shows the predicted spectra of the MM, IDM, and CM noise voltages with the filters. Fig.10 shows the measured spectra of the MM, IDM, and CM noise voltages with the filters by spectrum Analyzer Agilent E4411B (9 KHz–1.5GHz). In this paper, all EMI spectra displayed on the spectrum analyzer are employed by a peak detector and a 10-KHz resolution bandwidth. The agreement between the prediction and measurement illustrates that the information of impedances and voltage sources for a particular power converter is valid in predicting the actual EMI filter's effect. The circuit design was simulated using PSPICE; the schematic circuit is shown in Fig.11.

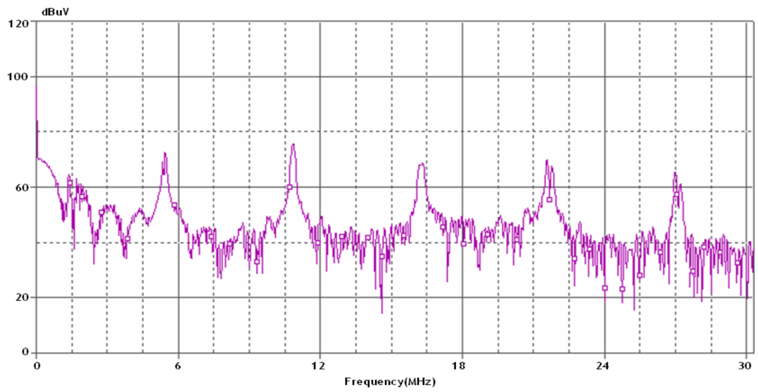

(a)

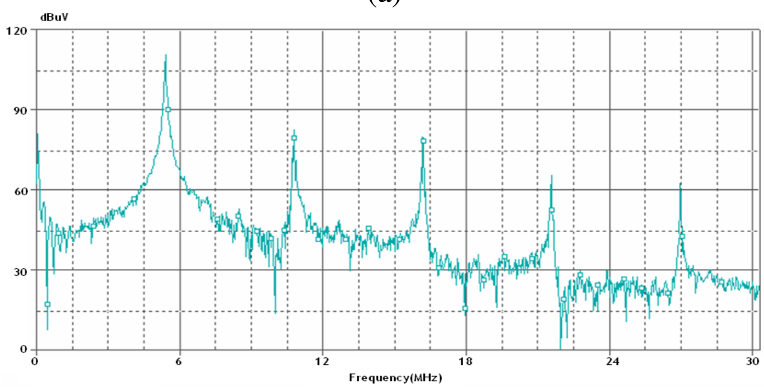

(b)

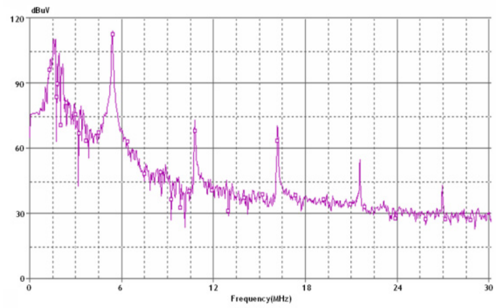

(c)

Figure 9: Predicted EMI spectra with filter. MM noise. (b) IDM noise. (c) CM noise.

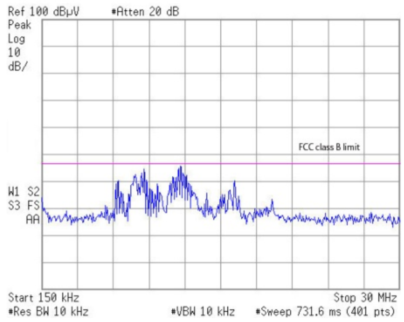

(a)

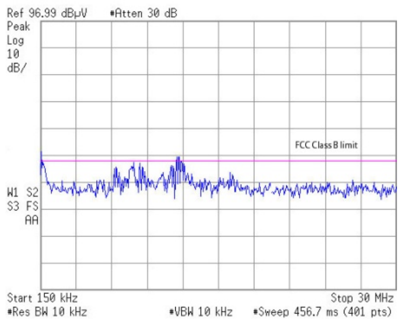

(b)

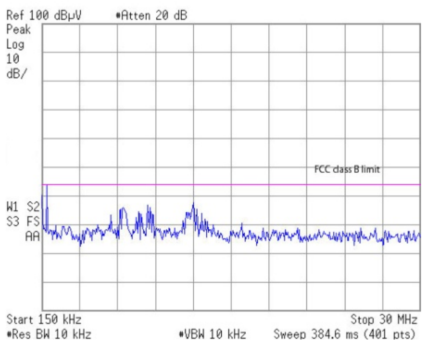

(c)

Figure 10: Measured EMI spectra with filter. (a) MM noise. (b) IDM noise. (c) CM noise.

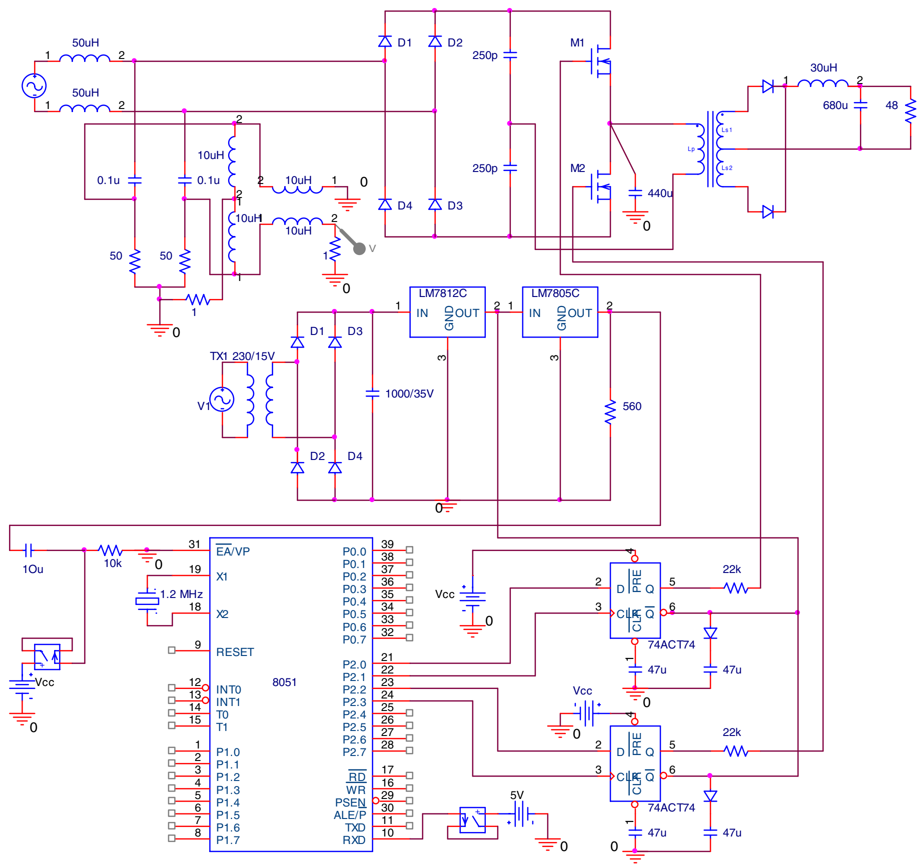

Figure 11: Schematic diagram of the simulation circuit.

Since the model is based on equivalent circuits, its validity is limited to frequencies below around 30 MHz. The proposed model provides a simple (yet adequate) means to make an initial estimation of the extent of the interference. The parameter values can never be estimated accurately. These results show that once the noise models are determined, the proposed method can be extended to investigate the effectiveness of filtering techniques. Table-II shows the simulation waveform results. Table-III shows the hardware waveform results. The simulated results are compared with hardware implementation results. The results obtained are satisfying the Federal Communications Commission (FCC) class B regulations.

Table II: Simulation Waveform Results.

Sl. No.	Frequency in MHz	Without Filter (dBμV)	With Filter (dBμV)		
			MM	IDM	CM
1	10	110	50	49	34
2	20	98	42	37	32
3	30	87	33	28	28

Table III: Hardware Waveform Results

Sl. No.	Frequency in MHz	Without Filter (dBµV)	With Filter (dBµV)		
			MM	IDM	CM
1	10	105	48	45	28
2	20	93	35	38	27
3	30	82	28	34	25

Fig.12 shows the hardware of the conducted EMI measurement for an isolated half-bridge ac–dc converter. A two way 0˚ combiner (ZFSC-2-6-75) and a two way 180˚ power combiner (ZFSCJ-2-1) are used to measure the CM, the IDM, or the MM noise via election of a three way built-in switch. Microcontroller is used to generate driving pulses for the MOSFETs.

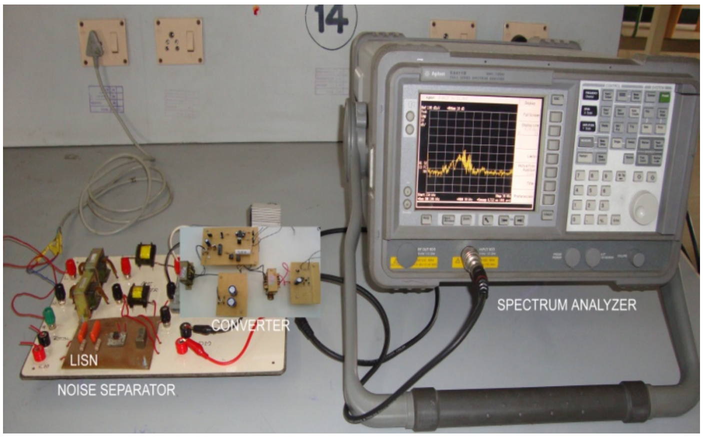

Figure 12: Photograph of the measurement arrangement.

Conclusion

Equivalent circuit modeling method is proposed to represent the conducted EMI coupling of a power converter. Three dominant modes of EMI noise coupling are analyzed and investigated, and the essential coupling models have been described for the noise coupling based on the measurements. Once the parameters of the EMI model are identified, the process can enable one to predict the actual attenuation of a particular EMI filter. The simulated results are compared with hardware implementation results. The results obtained are satisfying the FCC class B regulations The results contained in this paper can provide EMC designers with a useful tool to design EMI filters in power converters. The equivalent noise voltage sources as well as the coupling impedances were measured separately. Experimental Results have shown that the proposed method is very effective and accurate in identifying and capturing EMI features in switching power converters. The method presented is not only limited to half-bridge converters, but it can be applied to many different converter topologies, such as buck, flyback, boost, with single-phase diode bridge front-end. This model contains the salient features of conducted EMI, is convenient to use, and gives adequate prediction of EMI behavior in switching converters.

References

[1] L. Ran, "Conducted electromagnetic emissions in induction motor drive systems Part I: Time domain analysis and identification of dominant modes," IEEE Trans. Power Electron., vol. 13, no. 4, pp. 757–767, Jul. 1998.

[2] L. Ran, "Conducted electromagnetic emissions in induction motor drive systems Part II: Frequency domain models," IEEE Trans. Power Electron., vol. 13, no. 4, pp. 768–776, Jul. 1998.

[3] M. Jin, M. Weiming, P. Qijun, K. Jun, Z. Lei and Z. Zhihua, "Identification of essential coupling path models for conducted EMI prediction in switching power converters," IEEE Trans. Power Electron., vol. 21, no. 6, pp. 1795–1803, Nov. 2006.

[4] H. Zhu, Y. Tang, J.-S. Lai, and A. Hefner, "Characterization of power electronics system interconnect parasitics using time domain reflectometry," IEEE Trans. Power Electron., vol. 14, no. 4, pp. 622–628, Jul. 1999.

[5] H. Heeb and A. E. Reuhli, "Three-dementional interconnect analysis using partial element equivalent circuits," IEEE Trans. Circuits Syst., vol. 39, no. 11, pp. 974–982, Nov. 1992.

[6] C. Chen, "Characterizing the generation & coupling mechanisms of electromagnetic interference noise from an electric vehicle traction drive up to microwave frequencies," in Proc. IEEE Appl. Power Electron. Conf., 2000, pp. 1170–1176.

[7] L. Ran, J. C. Clare, K. J. Bradley, and C. Christopoulos, "Measurement of conducted Electromagnetic emissions in PWM motor drives systems without the need for an LISN," IEEE Trans. Electromag. Compat., vol. 41, no. 1, pp. 50–55, Feb. 1999.

[8] D. Gonzalez, J. Gago, and J. Balcells, "Analysis and simulation of conducted EMI generated by switched power converters: Application to a voltage source inverter," IEEE Trans. Ind. Electron., vol. 50, no. 6, pp. 801–806, Dec. 2003.

[9] N. K. Poon, B. Pong, J. Liu, and C. Tse, "Essential-coupling-path models for non-contact EMI in switching power converters using lumped circuit elements," IEEE Trans. Power Electron., vol. 18, no. 2, pp. 686–695, Mar. 2003.

[10] S. Brehaut, M. O. El Bechir, J.-C. Le Bunetel, D. Magnon, and A. Puzo, "Analysis EMI of a PFC on the band pass 150 kHz–30 MHz for a reduction of the electromagnetic pollution," in Proc. IEEE Appl. Power Electron. Conf., 2004, pp. 695–700.

[11] S. Brehaut, J. C. Le Bunetel, D. Magnon, and A. Puzo, "A conducted EMI model for an industrial power supply full bridge," in Proc. IEEE Power Electron. Spec. Conf., 2004, pp. 3227–3231.
[12] D. Zhang, "Non-intrinsic differential mode noise caused by ground current in an off-line power supply," in Proc. IEEE Power Electron. Spec. Conf., 1998, pp. 1331–1333.
[13] S. Qu and D. Chen, "Mixed-mode noise and its implications for filter design in offline switching power supplies," IEEE Trans. Power Electron., vol. 17, no. 4, pp. 502–507, Jul. 2002.
[14] M. Jin and M. Weiming, "A new technique for modeling and analysis of mixed-mode conducted EMI noise," IEEE Trans. Power Electron., vol. 19, no. 6, pp. 1679–1687, Nov. 2004.
[15] M. Jin and M. Weiming, "Power converter EMI analysis including IGBT nonlinear switching transient model," in Proc. IEEE ISIE'05, Dubrovnik, Croatia, Jun. 2005, pp. 499–504.
[16] F. Y. Shih, D. Y. Chen, Y. P. Wu, and Y. T. Chen, "A procedure for designing EMI filters for ac line applications," IEEE Trans. Power Electron., vol. 11, no. 1, pp. 170–181, Jan. 1996.
[17] S. Ye, W. Eberle, and Y.-F. Liu, "A novel EMI filter design method for switching power supplies," IEEE Trans. Power Electron., vol. 19, no. 6, pp. 1668–1678, Nov. 2004.